Shock wave shape on power law leading edges

W. F. N. Santos

Combustion and Propulsion Laboratory, National Institute for Space Research, Cachoeira Paulista, SP 12630-000 Brazil

Abstract. Computations using the Direct Simulation Monte Carlo method are presented for hypersonic flow on power law shaped leading edges. The primary aim of this paper is to examine the geometry effect of such leading edges on the shock wave structure. The sensitivity of the shock wave shape and shock standoff distance to shape variations of such leading edges is calculated by using a model that classifies the molecules in three distinct classes, i.e., undisturbed freestream molecules, molecules that had struck the surface of the leading edge, and molecules that had been indirectly affected by the presence of the leading edge. Calculations show that the shock wave shape is in surprising agreement with that predicted by the hypersonic small disturbance theory for the flow conditions considered.

1 Introduction

Hypersonic configurations are generally characterized by slender bodies and sharp leading edges in order to achieve good aerodynamic properties like high lift and low drag. Certain configurations, such as hypersonic waveriders, are designed analytically with infinitely sharp leading edges for shock wave attachment. Because the shock wave is attached to the leading edge of the vehicle, the upper and lower surface of the vehicle can be designed separately. Furthermore, this attached shock prevents spillage of higher pressure air from the lower side of the vehicle to the upper side. As a result of this attached shock, waveriders have been shown to have the potential to provide high values for the lift-to-drag ratio at high Mach numbers.

It is known that very sharp leading edge is not practical for a number of reasons: (1) it is difficult to manufacture, (2) some blunting is required for structural strength, and (3) the heat transfer to the nose is severe at high Mach numbers. In this context, any practical waverider will have some degree of bluntness dictated by either manufacturing or heating requirements. Coupled with viscous effects, the resulting shock wave will exhibit a standoff distance. In addition, shock wave detachment will allow pressure leakage from the lower surface of the vehicle to the upper surface, thereby degrading the aerodynamic performance of the vehicle.

Power law shaped leading edges ($y \propto x^n, 0 < n < 1$) may provide the required bluntness for heat transfer, manufacturing and handling concerns with reduced departures from ideal aerodynamic performance. This concept is based on work of Mason and Lee [1], who have pointed out, based on Newtonian flow analysis, that power law shapes exhibit both blunt and sharp aerodynamic properties. They suggested the possibility of a difference between shapes that are geometrically sharp and shapes that behave aerodynamically as if they were sharp.

The primary goal of this paper is to investigate the effect of the power law exponent on the shock wave structure over such leading edges. The flow conditions represent those experienced by a spacecraft at altitude of 70 km. High-speed flows under low-density

conditions deviate from a perfect gas behavior because of the excitation of the internal modes of energy. In such a circumstance, the degree of molecular non-equilibrium is such that the Navier-Stokes equations are inappropriate. Hence, a Direct Simulation Monte Carlo (DSMC) method is used to examine the shock wave structure for the idealized situation of rarefied hypersonic two-dimensional flow. Attention will be addressed to the analysis of the shape and position of the shock wave relative to the body producing it.

2   Leading-edge geometry definition

The power-law shapes are modelled by assuming a sharp leading edge of half angle θ with a circular cylinder of radius R inscribed tangent to this wedge. The power law shapes, given by $y = ax^n$, $0 < n < 1$, are also inscribed tangent to the wedge and the cylinder at the same common point where they have the same slope angle. It was assumed a wedge half angle of 10 deg, a circular cylinder diameter of 10^{-2}m and power law exponents of $1/2$, 0.6, $2/3$, 0.7, $3/4$ and 0.8. Figure 1(a) shows schematically this construction.

From geometric considerations, the power law constant a is obtained by matching slope on the wedge, circular cylinder and power law body at the tangency point. The common body height H at the tangency point is equal to $2R\cos\theta$, and the body length L from the nose to the tangency point in the axis of symmetry is given by $nH/2\tan\theta$.
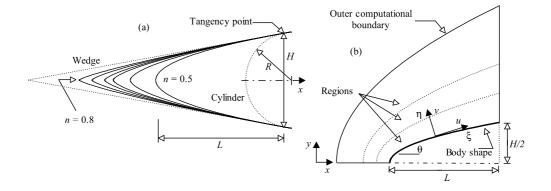

Fig. 1. (**a**) leading edge geometry and (**b**) the computational domain

3   Computational method and procedure

The degree of departure of a flow from the continuum is indicated by the flow Knudsen number, $Kn = \lambda/L$, where λ is the mean free path and L is the characteristic length of the flow. Traditionally, flows are divided into four regimes [2]: $Kn < 0.01$, continuum flow, $0.01 < Kn < 0.1$, slip flow, $0.1 < Kn < 10$, transitional flow, and $Kn > 10$, free molecular flow.

The most successful numerical technique for modelling complex flows in the transitional regime has been the Direct Simulation Monte Carlo (DSMC) method developed by Bird [3]. The DSMC method models the flow as being a collection of discrete particles, each one with a position, velocity and internal energy. The state of the particles is stored

and modified with time as the particles move, collide, and undergo boundary interactions in simulated physical space. The molecular motion and intermolecular collisions are uncoupled over the small time step used to advance the simulation. The time step ought to be sufficiently small in comparison with the local mean collision time [3].

The molecular collisions are modelled by the variable hard sphere (VHS) molecular model [4], and the energy exchange between kinetic and internal modes is controlled by the Larsen-Borgnakke statistical model [5]. The simulations are performed using a non-reacting gas model consisting of two chemical species, N_2 and O_2. Energy exchanges between the translational and internal modes are considered, and relaxation numbers of 5 and 50 were used for the calculations of rotation and vibration, respectively.

The flow field is divided into a number of regions, which are subdivided into computational cells, and the cells are further subdivided into subcells. The cell provides a convenient reference for the sampling of the macroscopic gas properties, and the subcell for the selection of the collision partners. The linear dimensions of the cells should be of the order of the local mean free path or even smaller [3]. The computational domain used for the calculations is made large enough so that the upstream and side boundaries can be specified as freestream conditions. The flow at the downstream outflow boundary is supersonic and vacuum conditions are specified [3]. A schematic view of the computational domain is depicted in Fig. 1(b). Advantage of flow symmetry is taken into account in order to reduce the computational domain. The grid generation scheme, the effect of grid resolution and the complete validation process employed in this study are described in Santos [6].

The freestream conditions used in the present calculations are those given by Santos and Lewis [7] and summarized in Table 1. The freestream velocity V_∞ is assumed to be constant at 3.5 km/s, which corresponds to freestream Mach number M_∞ of 12. The wall temperature T_w is assumed constant at 880 K. Also diffusion reflection with full thermal accommodation is assumed for the gas-surface interactions. The freestream Knudsen number, Kn_∞, corresponds to 0.0903, where the characteristic dimension was defined as being the diameter of the circular cylinder. Finally, the freestream Reynolds number by unit meter Re_∞ is 21455.

Table 1. Freestream conditions

T_∞(K)	p_∞(N/m^2)	ρ_∞(kg/m^3)	μ_∞(Ns/m^2)	n_∞(m^{-3})	λ_∞(m)
220.0	5.582	8.753×10^{-2}	1.455×10^{-2}	1.8209×10^{21}	9.03×10^{-4}

In order to investigate the shock wave structure, the flow is assumed to consist of three distinct classes of molecules: those molecules from the freestream that have not been affected by the presence of the leading edge are denoted as class I molecules; those molecules that, at some time in their past history, have struck and been reflected from the body surface are denoted as class II molecules; and those molecules that have been indirectly affected by the presence of the body are defined as class III molecules.

It is assumed that the class I molecule changes to class III molecule when it collides with class II or class III molecule. Class I or class III molecule is progressively transformed into class II molecule when it interacts with the body surface. Also, a class II molecule remains class II regardless of subsequent collisions and interactions. Therefore,

the transition from class I molecules to class III molecules may represent the shock wave, and the transition from class III to class II defines the boundary layer.

The molecule classification that has been adopted here was presented by Lubonski [8] in order to study the hypervelocity Couette flow near the free molecule regime. He divided the gas into three classes of molecules: "freestream", "reflected from the boundary" and "scattered". For the purpose of flow visualization, Bird [9] applied the same scheme of classification by identifying the classes by colors: blue for class I, red for class II and yellow for class III molecules.

4   Computational results and discussions

The purpose of this section is to discuss and to compare differences in the shock wave shape and shock wave standoff distance due to the variations in the body power law exponent.

In a rarefied flow, the shock wave has a finite region that depends on the transport properties of the gas, and can no longer be considered as a discontinuity obeying the classical Rankine-Hugoniot relations. Hence, the shape of the shock wave will be considered as being the center of the shock wave.

The distribution of molecules for each class along the stagnation streamline is presented in Figs. 2(a) (log scaling) and 2(b) (linear scaling) for the $n = 1/2$ case. η/λ_∞ is the dimensionless distance away from the body (see Fig. 1(b)), and f is the ratio of the number of molecules for each one of the classes to the total amount of molecules inside each cell.
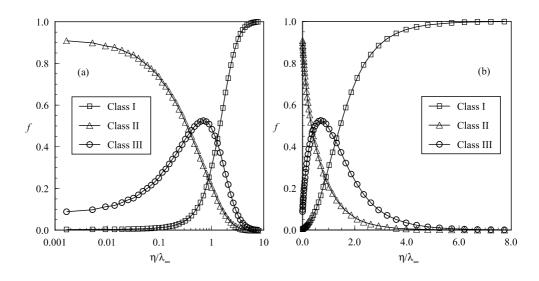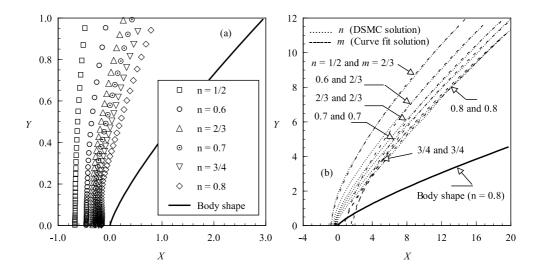

Fig. 2. Distribution of molecules for classes I, II and III along the stagnation streamline: (**a**) log scaling, and (**b**) linear scaling

The shock wave center is obtained by calculating the position that corresponds to the maximum f for class III molecules in the η-direction along the body surface (see Fig. 1(b)). Figure 3(a) illustrates the shock wave shapes in the vicinity of the stagnation

region. X and Y are the cartesian coordinates x and y normalized by λ_∞. For comparison purpose, only the body shape for the $n = 0.8$ case is shown.

Fig. 3. (a) Computational results for shock wave shape in the vicinity of the stagnation region, and (b) shock wave shape curve fits on various body power law shapes

Lees and Kubota [10] pointed out that flow similarity is possible for a class of bodies of the form x^n. In the more general case for $0 < n < 1$, the shock wave grows like x^m. When n grows from zero, m begins by keeping the constant value $m = 2/3$, and if n keeps on growing towards, m remains equal to n. The similarity solutions are obtained by assuming the hypersonic slender body approximations [11]. As a result, they are not valid near the nose of the leading edge where the approximations are violated. At or near the nose, the surface slope, the curvature and higher derivatives are infinite and, therefore, the similarity solutions breakdown. Hence, a fitting process is performed over the coordinate points yielded by DSMC simulations in order to approximate the shock wave shapes by the form, $y = A(x+B)^m$, where A is the power law constant of the curve fit, B is the distance from the nose of the leading edge, and m is the power law exponent of the curve fit, i.e., the shock wave power law exponent.

In order to compare the shock wave shapes obtained in this work with those predicted by Lees and Kubota [10], curve fit solutions are found by keeping $m = 2/3$ for $n \leq 2/3$ cases, and $m = n$ for $n > 2/3$ cases. Hence, n and m stand for body and shock wave power law exponents, respectively. It is worthwhile to note that the shock wave shape is not predicted by the theoretical solution close to the nose of the leading edges, since the hypersonic slender body approximations are violated there. In this context, the fitting process is performed over the coordinate points located far from the stagnation region (say $x/\lambda_\infty > 5.0$), where it is expected that the blunt nose effects are no more important.

Figure 3(b) displays the curve fit solutions for shock wave shape over various power law body shape. In this figure, n represents the shock wave yielded by the DSMC solution and m the curve fit solution. As can be seen, the DSMC solution presents remarkable agreement with the power law exponents of the curve fit predicted by the analytical

solution [10]. As would be expected, the curve fitting solution deviates from the DSMC solution close to the nose of the leading edge.

The shock wave standoff distance, defined as being the distance between the shock wave center and the nose of the leading edge, along the stagnation streamline, can be observed in Fig. 3(a). The shock standoff distance δ, normalized by λ_∞, is 0.689, 0.460, 0.333, 0.286, 0.214, and 0.159 for power law exponents of 1/2, 0.6, 2/3, 0.7, 3/4, and 0.8, respectively. It is seen that the shock standoff distance decreases as n increases, as would be expected.

The shock standoff distance becomes important in hypersonic vehicles such as waveriders, which depend on leading edge shock attachment to achieve their high lift-to-drag ratio at high lift coefficient. In this context, the power law leading edges seem to be more appropriate than the reference circular cylinder ($\delta/\lambda_\infty = 1.646$), since they present reduced shock wave detachment distances. Nevertheless, smaller shock detachment distance is associated with a higher heat load to the nose of the body (Santos and Lewis [7]).

5   Concluding remarks

This study applies the Direct Simulation Monte Carlo method to assess the impact on the shock wave structure due to variations in the shape of power law leading edges. The calculations provided information concerning the nature of the shock wave shape and shock wave detachment distance resulting from variations in the body shape for the idealized situation of two-dimensional hypersonic rarefied flow.

The computational results indicated that the shock wave shape grows like x^m for power law leading edges. The shock wave shape confirmed the finding predicted by the hypersonic small disturbance theory in that the shape of the shock wave follows the shape of the body far from the nose of the leading edge, provided the body power law exponent is larger than 2/3.

References

1. W. H. Mason, J. Lee: J. of Spacecraft and Rockets **31**, 378 (1994)
2. S. Schaff, P. Chambre: *Fundamentals of Gas Dynamics*, 1st edn. (Princeton University Press, Princeton, NJ, 1958)
3. G. A. Bird: *Molecular Gas Dynamics and the Direct Simulation of Gas Flows*, 2nd edn. (Oxford University Press, Oxford, England, UK, 1994)
4. G. A. Bird: 'Monte Carlo Simulation in an Engineering Context'. In: *Progress in Astronautics and Aeronautics: Rarefied Gas Dynamics*, ed. by Sam S. Fisher (AIAA, New York 1988) vol. 74, pp.239–255
5. C. Borgnakke, P. S. Larsen: J. of Computational Physics **18**, 405 (1975)
6. W. F. N. Santos: 'Direct Simulation Monte Carlo of Rarefied Hypersonic Flow on Power Law Shaped Leading Edges'. PhD Thesis, University of Maryland, College Park, MD, (2001)
7. W. F. N. Santos, M. J. Lewis: J. of Spacecraft and Rockets **39**, 917 (2002)
8. J. Lubonski: Archiwum Mechaniki Stosowanej **14**, 553 (1962)
9. G. A. Bird: J. of Fluid Mechanics **36**, 571 (1969)
10. L. Lees, T. Kubota: J. of the Aeronautical Sciences **24**, 195 (1957)
11. M. D. Van Dyke: 'A Study of Hypersonic Small-Disturbance Theory'. NACA TN-3173 (1977)